Of mice and men: topologically complex dendrites assemble uniquely human networks

Lida Kanari*[1], Ying Shi[1], Alexis Arnaudon[1], Natalí Barros-Zulaica[1], Ruth Benavides-Piccione[2], Jay S. Coggan[1], Javier DeFelipe[2], Kathryn Hess[3], Huib D. Mansvelder[4], Eline J. Mertens[4], Julie Meystre[5], Rodrigo de Campos Perin[5], Maurizio Pezzoli[5], Roy Thomas Daniel[6], Ron Stoop[7], Idan Segev[8], Henry Markram[1] and Christiaan P.J. de Kock[4]

[1]Blue Brain Project, École Polytechnique Fédérale de Lausanne (EPFL), Campus Biotech, 1202 Geneva, Switzerland.

[2]Laboratorio Cajal de Circuitos Corticales, Universidad Politécnica de Madrid and Instituto Cajal (CSIC), Pozuelo de Alarcón, Madrid 28223, Spain

[3]Laboratory for Topology and Neuroscience, Brain Mind Institute, École Polytechnique Fédérale de Lausanne (EPFL), 1015 Lausanne, Switzerland

[4]Department of Integrative Neurophysiology, Center for Neurogenomics and Cognitive Research, Vrije Universiteit Amsterdam, 1081 HV Amsterdam, the Netherlands

[5] Laboratory of Neural Microcircuitry, École Polytechnique Fédérale de Lausanne (EPFL), 1015 Lausanne, Switzerland

[6] Department of Clinical Neurosciences, Neurosurgery Unit, Centre Hospitalier Universitaire Vaudois, Lausanne, Switzerland

[7] Center for Psychiatric Neurosciences, Department of Psychiatry, Lausanne University Hospital Center, Lausanne, Switzerland

[8] Department of Neurobiology and Edmond and Lily Safra Center for Brain Sciences, The Hebrew University of Jerusalem, 9190501 Jerusalem, Israel

* Corresponding author: lida.kanari@gmail.com

Abstract: The organizational principles that distinguish the human brain from other species have been a long-standing enigma in neuroscience. Focusing on the uniquely evolved cortical layers 2 and 3 in human, human pyramidal neurons show more intense connectivity among themselves compared to the mouse. This is surprising because human L2 and 3 neurons are much sparser. We show that the number and size of neurons *per se* fail to account for this connectivity difference, suggesting that another property of neurons is key in determinant of human network connectivity. Topological comparison of dendritic structure reveals much higher perisomatic (basal and oblique) branching density in human pyramidal cells. Using topological tools we quantitatively show that this cellular-level structural property directly impacts network-level topological complexity, including the formation of a rich subnetwork structure. We conclude that greater dendritic complexity, which is a defining attribute of human L2 and 3 neurons, may provide enhanced computational capacity and cognitive flexibility to the human cortex.

Keywords: Human; Rodent; Mouse; Neuron morphology; Topological complexity; Networks; Pyramidal cell

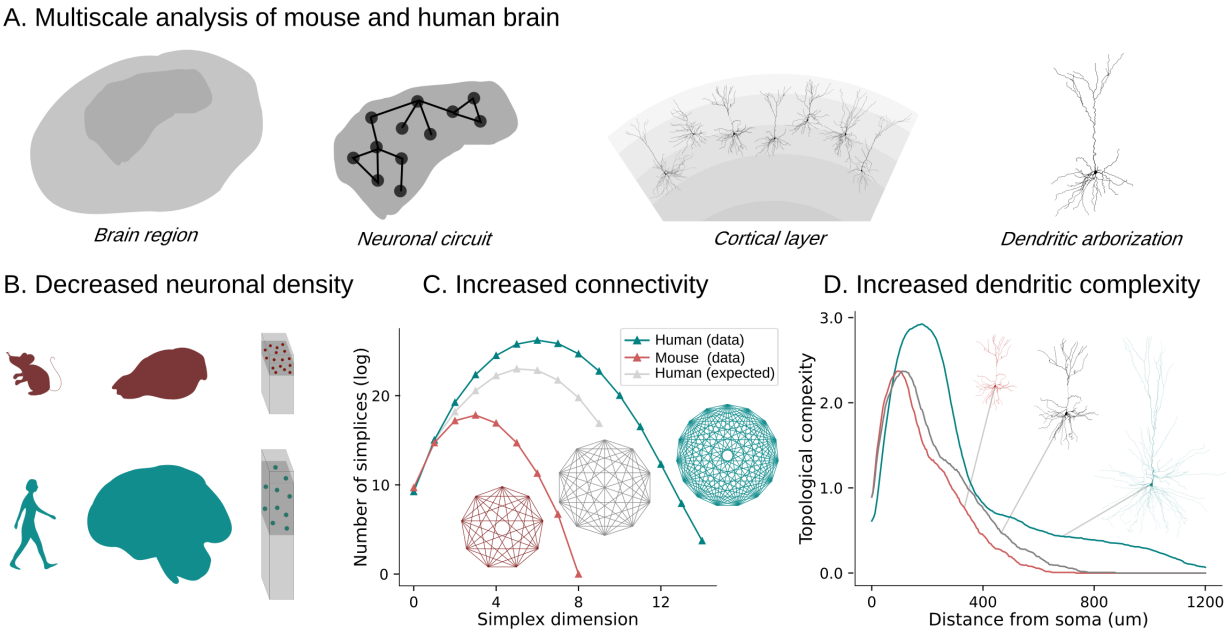

Graphical abstract. A. Multiscale analysis was performed to compare the mouse and human brains: from the anatomical properties of brain regions to the morphological details of single neurons. B. Human circuits are larger than mice in terms of size and number of neurons, but present descreased neuron density, resulting in increased distances between neurons, particularly among pyramidal cells. C. Greater network complexity emerges within the human brain. Network complexity is defined by larger groups of neurons forming complex interconnections throughout the network. D. The topological analysis of layer 2/3 pyramidal cells in the cortex reveals an intriguing difference: human neurons exhibit a significantly larger number of dendritic branches, especially near the cell body compared to mice. This phenomenon is termed "higher topological complexity" in dendrites. Our findings suggest that dendritic complexity wields a more substantial influence on network complexity than neuron density does, hinting at a potential strategy for enhancing cognitive abilities.

Introduction

The question of how the brain contributes to human cognition has been a topic of debate and discussion since ancient times. The shift from Aristotle's belief that intellect resided in the heart to Gallen's assertion of the brain's significance in ancient Rome marked a pivotal moment in this ongoing discourse. Humans have long been intrigued by the reasons behind their own relative sophistication compared to other animals (1), sparking deep curiosity about the unique capabilities of the human brain. Initially, it was postulated that human cognitive prowess was linked to the sheer magnitude of our brains (1), stemming from the notion that intelligence is directly correlated with brain size. However, research has failed to identify similar abilities in other large-brained animals, such as elephants (2) and cetaceans (3). Furthermore, subsequent studies (4) systematically analyzing the ratio of brain to body mass refuted these theories, demonstrating that human brain size is not distinctive compared to other animals. Nevertheless, the conviction that the human brain is exceptional among mammalian brains persists, as indicated by the numerous studies that investigate possible correlations of human intelligence with larger cell counts (5), cortical thickness (6; 7), increased cortical folding (8) or dendritic size (9). However, despite extensive endeavors to unravel its mysteries, numerous aspects of our unique characteristics remain elusive. While there may well be other factors at play in defining human intelligence, in this study we demonstrate that the shapes of dendrites are an important indicator of network complexity that cannot be disregarded in our quest to identify what makes us human.

Santiago Ramon y Cajal sparked the intriguing question of the possible presence of distinctive structural characteristics in human neurons that contribute to their optimal functioning when compared to neurons in other species (10). Numerous studies have examined the unique functional, molecular, and structural features of human neurons (11; 12; 13). However, it is only recently that significant progress has been made in addressing the knowledge gap concerning distinctive features of human neurons by integrating multimodal datasets that encompass single neuron morphologies, neurochemistry, electrophysiology, and transcriptomics (14; 15; 16; 17). Several laboratories (12; 13; 18; 15) have contributed valuable insights into the structural properties of human neurons by generating morphological reconstructions. In parallel, detailed electron microscopy (EM) reconstructions of human brain tissue (19; 20; 21; 22) have provided important information regarding the composition and connectivity properties of human neurons. These recent advancements in data generation are enabling a more comprehensive exploration of the intricate structural properties of human neurons and their potential implications for neural function.

In this study, we leveraged these invaluable resources to create a large collection of neurons, normalized with respect to orthogonal factors, such as age, brain region and cortical thickness. An assiduous analysis of the anatomical properties of the cortex, based on dense tissue reconstructions (21) and detailed anatomical studies (11; 23) indicated a significantly lower cell density in the human cortex, leading to greater inter-neuron distances. Putting

together the anatomical properties of the mouse and human cortex (11; 23; 21) and the experimental reconstructions of pyramidal cells in layers 2 and 3 of mouse and human cortex, we generated representative networks and studied their topological properties (24). Our investigation revealed that the combination of lower neuronal density and the unique morphological properties of human neurons resulted in a considerable increase in the number of directed simplices (25; 24) within the subnetworks of human pyramidal cells, suggesting the presence of abundant, strongly connected subnetworks within the human cerebral cortex. We therefore embarked on a thorough investigation to unravel the underlying factors and discern the distinctive features of human pyramidal cells that result in these significant differences in network complexity between species.

In order to maintain the neuropil density within the cortical tissue, despite the greater inter-neuronal distances, individual neurons must possess greater dendritic length. This hypothesis was initially proposed based on old histological studies (by Franz Nissl and Constantin Von Economo), suggesting that the wider separation of neurons in humans, compared to other species, could indicate a higher level of refinement in the connections between neurons (26). Through a meticulous morphological investigation, we corroborated previous findings (12; 18) indicating that human neurons exhibit greater total length and extend further from the soma. However, we established that size scaling (14), whether uniform or not, fails to adequately account for the observed increased connectivity in the subnetworks of human pyramidal cells. Our topological analysis (27) unveiled a distinctive pattern of high branching density surrounding the soma in human neurons, a trait absent in the mouse cortical dendrites. These results were found to be consistent across other cortical layers (e.g., layer 5) and brain regions (e.g., hippocampus), implying that this topological difference may be a universal feature distinguishing human pyramidal cell morphologies from those of mouse. This distinctive property proved pivotal in elucidating the observed network disparities. The distribution of additional dendritic branches in close proximity to the soma confers the advantageous ability to fill the inter-neuronal space, while preserving the connection probability between neurons and forming strongly connected cortical subnetworks of pyramidal cells. In addition, the abundance of these strongly connected pyramidal cell cliques necessitates the over-expression of inhibitory neurons, which regulate the cortical excitation through local subnetworks.

The findings of our study suggest that a fundamental geometric principle underlies the observed variations in neuronal characteristics, which in turn has significant implications for the structural organization of human networks. Specifically, human networks exhibit a preference for greater complexity of individual cells, as opposed to the greater neuron density observed in mouse networks. This seemingly straightforward yet powerful distinction raises the intriguing question whether the augmentation of complexity within network nodes (i.e., dendrites) confer a cognitive advantage compared to increasing the number of nodes (i.e., neurons). While the necessary data to fully answer this question are not readily available, it is reasonable to speculate that the combination of highly complex dendrites and strongly

connected networks contributes to the high capacity for information processing of the human brain. These findings shed light on mechanisms underlying the exceptional cognitive abilities exhibited by humans and highlight the significance of considering the interplay between neuronal complexity and network organization in understanding brain function.

Results

Human cortex has lower neuronal density and larger inter-neuron distances

Contrary to previous assumptions, the size of the brain is not a proxy for the number of neurons it contains (5). In particular, despite the increase in cell counts observed in the human brain (11), the lower neuron density in the human cortex ($\approx 25,700/mm^3$) compared to the mouse cortex ($\approx 137,600/mm^3$) challenges this notion (Fig 1A-B). Another important difference is the significantly higher proportion of interneurons (Fig 1C), i.e. inhibitory neurons with local dendrites, comprising 30% of human neurons compared to a mere 12% in the mouse (26; 21).

In order to investigate the effect of lower neuron density on the spatial distribution of neurons, we computed the distance between the cells, assuming a uniform distribution of neurons within the cortical layers 2 and 3. The closest neighbor distance between human neurons is $\approx 19\mu m$, which is nearly twice that of mice at $\approx 11\mu m$ (see Methods: Computation of inter-neuron distances, Fig 1A). This difference is more striking when computed for pyramidal cells (closest neighbor pyramidal cell distance is $\approx 21.3\mu m$ in human versus $\approx 11.5\mu m$ in mouse), as opposed to the distance between interneurons, which is $\approx 28.5\mu m$ in human versus $\approx 22\mu m$ in mouse, due to the higher proportion of interneurons in the human cortex (Fig 1C-D).

We then computed the expected neuropil densities of dendritic branches within the tissue of the two species. For this experiment, we used the number of synapses ($11.8 \times 10^8/mm^3$ in human versus $26.56 \times 10^8/mm^3$ in mouse) within a volume of $1mm^3$ of the cortex (11) and the reported synaptic densities (21), $0.88/\mu m$ in human versus $2.15/\mu m$ in mouse). This analysis revealed that the total length of dendrites per cubic millimeter is comparable between the two species, with human dendrites measuring $\approx 1,340m/mm^3$ compared to $\approx 1,240m/mm^3$ in mice (Fig 1E), despite their significant differences in cell density ($25.7K$ neurons $/mm^3$ in humans versus $137.6K$ neurons $/mm^3$ in mouse). These observations imply that the total dendritic length is increased in human neurons, as is indeed observed by the larger size of human arborizations (Fig 1F) from the first available datasets (12; 13).

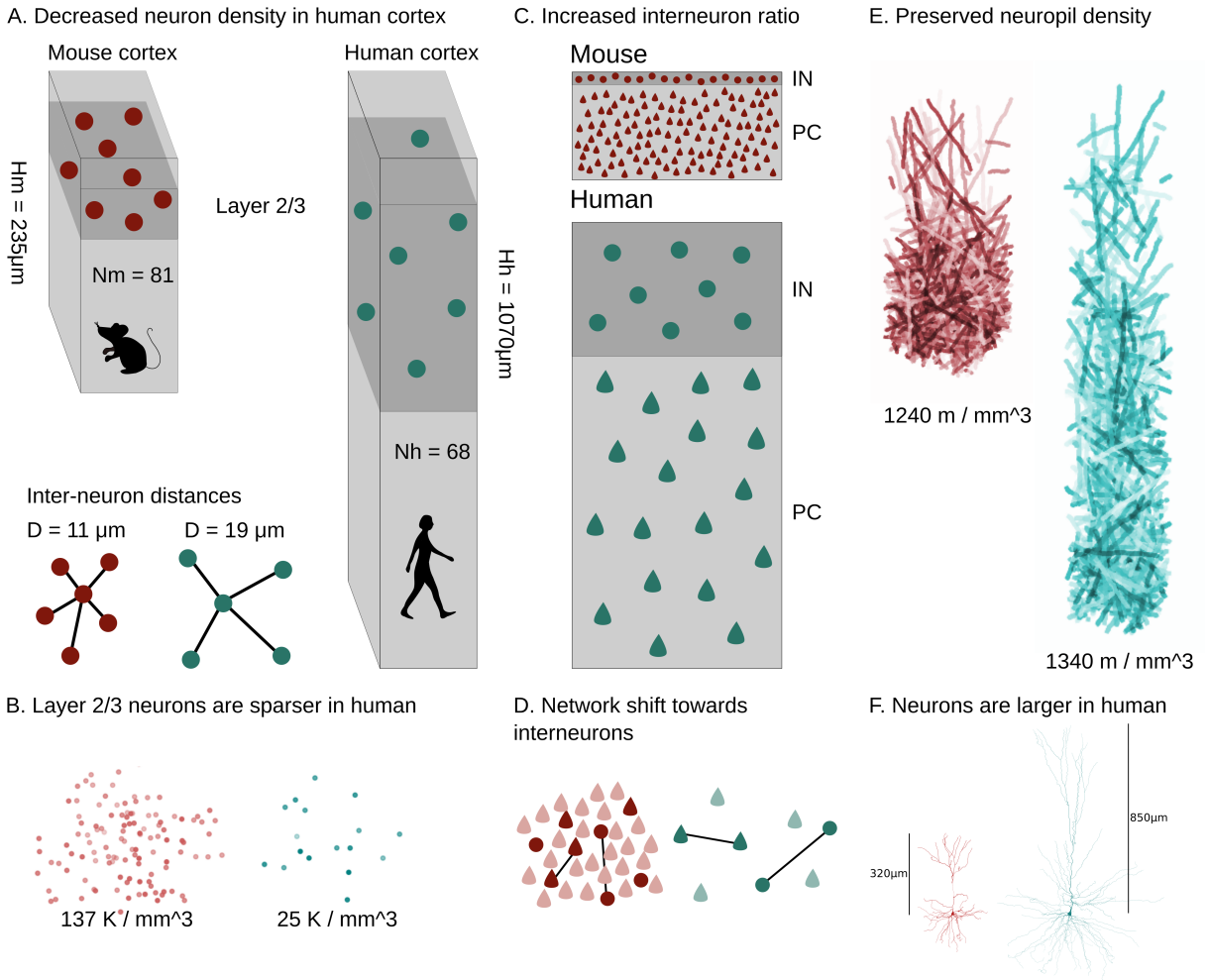

Figure 1: **Comparative analysis of network architecture.** A. Lower neuron density in human cortex leads to increased inter-neuron distances (almost double in human). B. Neurons are sparser in human networks. C. The percentage of interneurons increases in human cortex, indicating a significant network difference between species. D. The increased interneuron density changes the balance of inhibition / excitation in the network. E. The neuropil density (dendrites shown) is preserved between species. F. Human neurons are larger with more extended dendrites, as expected by the larger cortical thickness and lower neuronal density.

Human pyramidal cells generate strongly connected subnetworks

In order to understand how the anatomical differences between the two species contribute to the network architecture, we generated mouse and human networks and studied their structural connectivity. This analysis revealed significant differences between the two species. Using available data on neuronal densities (11) and the ratio of excitatory to inhibitory

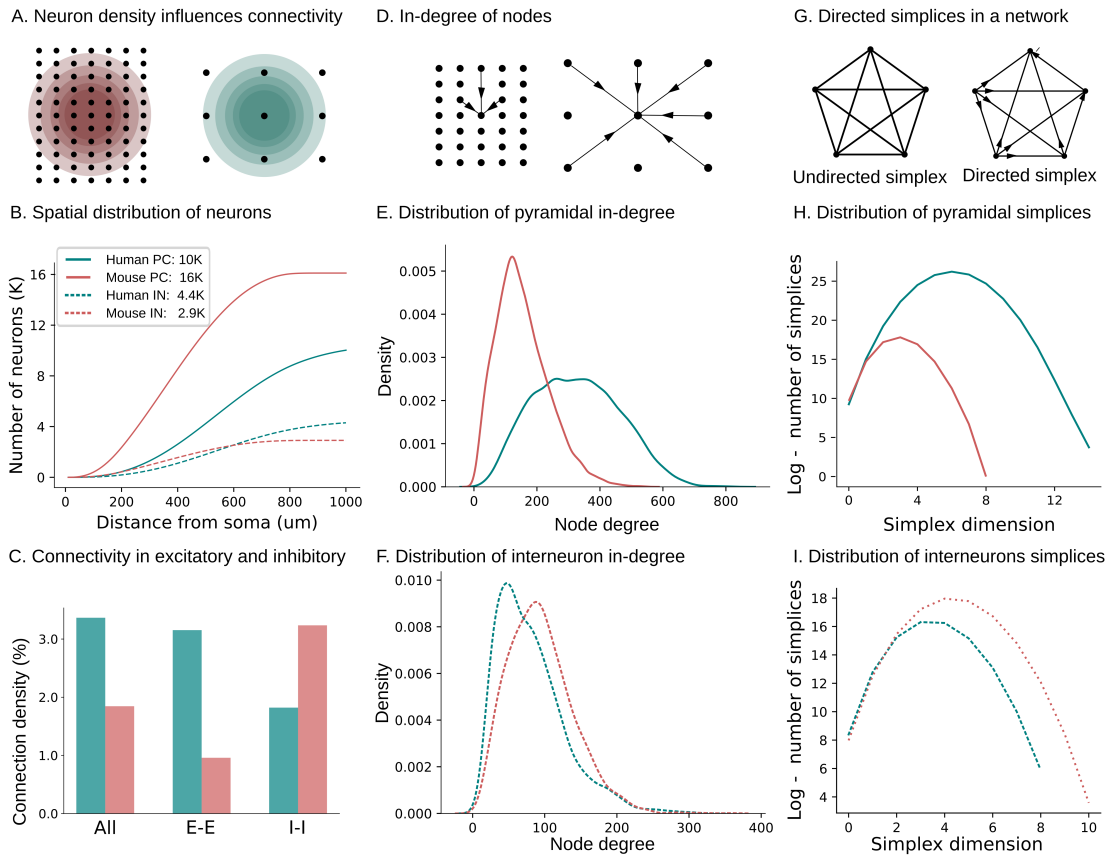

Figure 2: **Human pyramidal cells generate strongly connected subnetworks.** A. Grid illustrating differences in neuron density in human (teal) and mouse (red). Concentric spheres surrounding a central neuron portray the cell counts presented in (B). B. Number of neighbors. A cortical layer 2/3 of dimensions $1mm$ x $1mm$ was simulated for the respective cortical thickness of mouse ($235\mu m$) and human ($1070\mu m$) and the respective neuron counts for mouse ($28K$) and human ($18K$). The number of neurons at different distances ($0-1000\mu m$) from a central neuron was computed. Insert reports total cell counts. Note that cell counts do not linearly correspond to cell density due to the differences in the cortical thickness of the two species, which results in a larger cortical volume in the human cortex. C. Connectivity density (number of edges over maximum possible number of edges) for all neurons, and subnetworks of pyramidal cells and interneurons. D. Schematic of node in-degree for mouse and human networks. E. Distribution of in-degrees for human (teal) and mouse (red) pyramidal cells subnetworks. F. Distribution of in-degrees for human (teal) and mouse (red) interneuron subnetworks. G. Example of a five-simplex in undirected and directed graphs. H. Distribution of simplices for subnetworks of pyramidal cells. Log-scale is used for the number of simplices to depict the 3 orders of magnitude higher simplex counts in human. I. Distribution of simplices for subnetwork of interneurons.

neurons (21), along with morphological reconstructions for four different cell types (human pyramidal cells, mouse pyramidal cells, human interneurons, and mouse interneurons, see SI: Datasets), we computed the connectivity of the simulated human and mouse networks. It is important to note that the connectivity was determined through a random selection of 50% of all the appositions, i.e. touched between dendrites and axons, and thus, no direct comparison can be made to the connectivity measurements observed in actual biological circuits.

First we analyzed the spatial distribution of neurons in the two species (Fig 2A-B). Neurons were distributed homogeneously according to the respective neuron densities. The number of neurons found at different distances ($0-1000\mu m$) from a central neuron was computed (Fig 2B) and demonstrates that fewer neighbors are localized around a human neuron, as expected due to the lower neuronal density in the human cortex. The connectivity density, i.e., the ratio between the actual connections in the network over the maximum number of possible connections (equal to the square of number of nodes), of the human pyramidal cells subnetwork (Fig 2C) is much higher than the respective subnetwork in mice. On the other hand, the respective connectivity density of the human interneuron subnetwork is lower, despite the higher percentage of interneurons in the human cortex (30% in humans versus 12% in mice). In addition, the in-degree distribution(Fig 2D) in the subnetwork of human pyramidal cells also demonstrates a significant increase compared to the mouse subnetwork (Fig 2E). These results do not generalize to the subnetworks of interneurons which exhibit similar in-degree distributions between mouse and human (Fig 2F). The increase in the connectivity density and the in-degrees in the subnetwork of human pyramidal cells comes as a surprise to the reduced density of pyramidal cells in the respective cortical volume.

The complexity of the networks was assessed by computing the distribution of directed simplices (24). Simplices provide a comprehensive representation of fully connected subgraphs within the networks (Fig 2D), combining information about the density and the degree distribution of the graphs and represent network hubs that are related to modulation of cortical dynamics (28). Furthermore, it is worth noting that higher-dimensional simplices are associated with increased robustness in networks (29), since information can be efficiently transmitted in a specific direction, as all edges within the simplices are aligned to transmit information in the same direction. Surprisingly, despite the lower neuronal density observed in the human layer 2/3 cortex, the subnetwork of pyramidal cells exhibited a complex connectivity pattern, leading to the formation of higher-dimensional simplices. Specifically, in the human network, we observed simplices of dimension 15, whereas, in the mouse network, the dimension was limited to 9 (Fig 2H). The number of simplices in the human network was approximately three orders of magnitude larger compared to the mouse network. These findings suggest that the human cortical network displays a greater degree of complexity than its mouse counterpart, despite the lower neuronal density. These results do not generalize to the network of interneurons (Fig 2I), despite the larger inhibition / excitation ratio in human. Interneuron subnetworks, which express lower density of interneurons (cell counts

per volume) in human ($7.7K/mm^3$ in human versus $16.5K/mm^3$ in mouse), exhibit lower dimensional simplices (9 in humans versus 11 in mice) and smaller simplex counts (Fig 2I). Our results suggest that human cortical networks consist of an abundance of spatially sparse high-dimensional directed cliques of pyramidal cells which are controlled by localized dense inhibitory subnetworks of interneurons.

Simple dendritic scaling cannot explain species-specific phenotypes

We then investigated which morphological features can explain the significant increase in neuronal connectivity in human networks. We evaluated whether a simple scaling law can determine the relationship between the dendrites of the two species. Based on the observed variations in neuron size (14) and the conserved molecular cell types (30; 15; 16) across different species, the existence of a simple scaling law governing morphological cell types has been hypothesized. Due to the observed differences in body size, which results in larger human brains and increased cortical thickness (Fig 3A), it is assumed that the larger cell counts and the increased dendritic lengths can explain the enhanced cognitive abilities of humans (9).

We collected morphologies from diverse sources (12; 13; 18; 15) and ensured the coherence of the datasets by comparing their variation against the within-group variation. Neurons were selected exclusively from analogous brain regions and within comparable age ranges. The datasets employed for our analysis consisted of mouse and human pyramidal cells (from the temporal cortex (layers 2, 3 and 5) and hippocampus and interneurons from the layers 2 and 3 cortex (see SI: Datasets, Table S 1). Initially, we focused on pyramidal cells from layers 2 and 3. The clustering of human neurons and scaled mice neurons to compensate for the difference in cortical thickness between the two species (Fig 3B) demonstrates that cortical thickness alone cannot explain the observed morphological differences. A comprehensive comparative analysis of morphological characteristics between the pyramidal cells of cortical layers 2 and 3 of the two species revealed profound differences between human and mouse neurons (Fig 3C) and confirmed findings reported in previous studies (13; 18). Human pyramidal cells are larger, evidenced by their increased total lengths both in apical ($5975 \pm 2697\mu m$ in human apical dendrites, versus $2647 \pm 1047\mu m$ in mice) and basal dendrites ($5616 \pm 4000\mu m$ in human basal dendrites, versus $3127 \pm 1047\mu m$ in mice). In addition, human neurons extend to larger distances ($698 \pm 276\mu m$) compared to mouse ($349 \pm 96\mu m$) due to the increased thickness of the human cortex (2.2 times larger) and particularly layers 2/3 (4.5 times larger in human. Additionally, human apical dendrites possess more branches (53 ± 19 in humans, versus 35 ± 11 in mice). The detailed morphological analysis is summarized in Tables S 2-S 5.

A computation of pairwise connectivity at varying distances between pre-synaptic and post-synaptic cells (Fig 3D) shows a higher number of appositions, i.e., touches that can potentially become synapses, in human cells than in mouse cells. Surprisingly, when a similar analysis was conducted on mouse cells scaled to twice their original extents, fewer

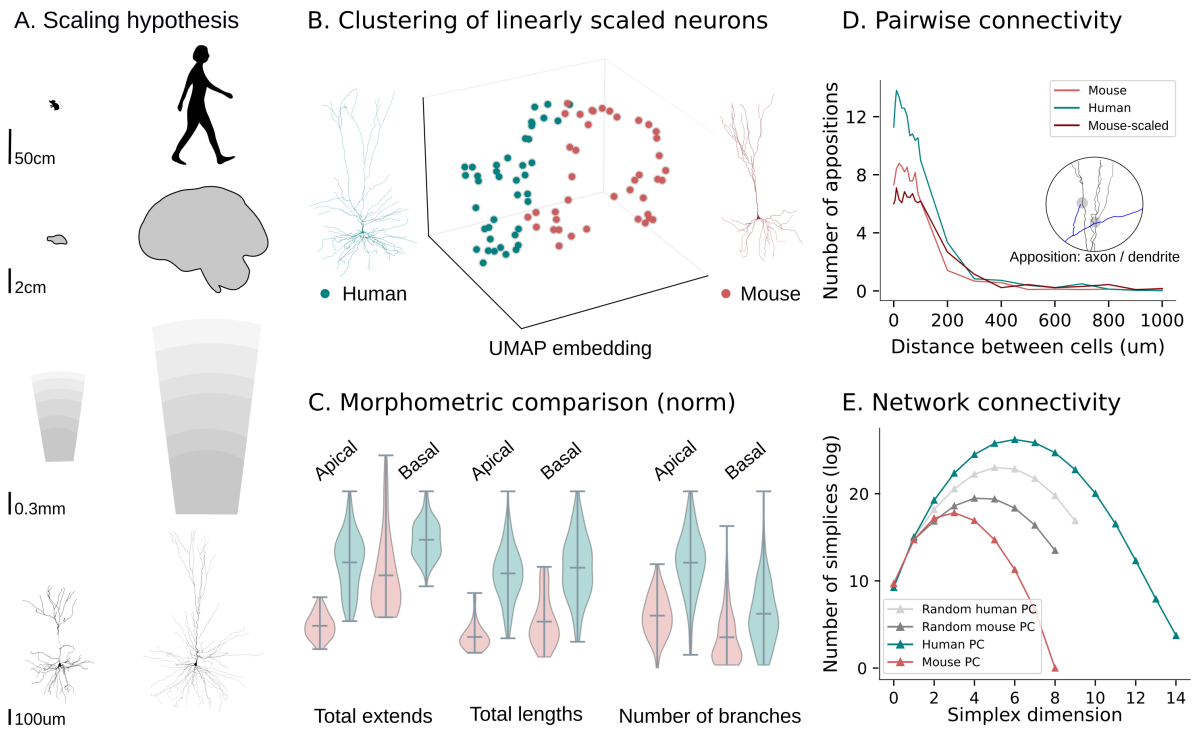

Figure 3: **Simple scaling cannot explain species-specific phenotypes.** A. Schematic representation of the scaling hypothesis: the dendritic size scales with the brain size, which in turn scales with the body size. B. The UMAP embedding of the topological representations (normalized to the same total size) of human (teal) and mouse (red) neurons shows a distinction between the two species. C. Comparison of pyramidal cell morphonetrics (normalized by macimum value in human, separated in apical and basal dendrites) show that morphological features do not scale uniformly. D. Pairwise number of appositions at different inter-neuron distances for pairs of mouse (red), human (teal) and scaled mouse (deep red) neurons. E. Log of simplex distribution for pyramidal cell networks of mouse (red) and human (teal) are compared to random Watts- networks of the same number of nodes and connectivity density (dark-gray: random network with mouse network properties, light-grey:random network with human network properties). The human networks are more complex than the equivalent random networks, as opposed to mouse networks which are less complex.

appositions were observed, an effect that can be attributed to the increased empty space between branches. Therefore, the increased total lengths of dendrites cannot sufficiently explain the observed connectivity differences. We hypothesize that the spatial arrangement of branches and their organization around the soma are important determinants of neuronal connectivity.

We then evaluated the effect of the increased number of neurons in the cortex as as a de-

terminant of the increased network complexity. We generated random small world networks (Watts-Strogats with probability $p = 0.6$) with the corresponding structural properties of the networks of pyramidal cells (number of nodes and connection density) and compared them to the reconstructed networks with similar properties (Fig 3E). This analysis indicates that network size (number of nodes and connectivity density) cannot sufficiently explain the observed network complexity as the human network shows higher complexity that the equivalent random network, while the mouse network shows lower complexity.

Topological profiles of layer 2 and 3 pyramidal cells show species-specific morphological traits

In order to identify the precise morphological features that are unique in each species, we studied the topological properties of neurons. The topological morphology descriptor, TMD (27), which encodes the topology of branches at different path distances from the soma, was used to study how branches are distributed in the two species. The extracted topological barcodes of the human (see Fig S 1) and mouse (see Fig S 2) pyramidal cells unveiled a fundamental difference in their branching patterns (Fig 4D-E). In the vicinity of the soma, human dendrites exhibit a higher density of branches (Fig 4H), which were also found to be longer than their mouse counterparts (Fig 4I). Specifically, collateral dendritic branches of human pyramidal cells start closer to the soma ($200 - 400\mu m$, Fig 4F) but extend to larger radial distances, thus conferring a distinct topological profile of longer branches close to the soma in human neurons.

We attempted to approximate the experimental data by employing an optimization algorithm to minimize the distances between mouse and human persistence barcodes. However, neither uniform nor non-uniform scaling (see Fig 4J-K, Methods: Scaling optimization) could adequately fit the experimental data. The persistence diagrams, normalized for cell sizes between $0-1$, were approximated by a Gaussian kernel (three centers, Fig 3G) in both species. The distinct dendritic density patterns observed at different distances from the soma are specific to each species, as evidenced by the spatially distinct differences between the approximated gaussian kernels. Species specific topology explains why simple scaling laws cannot sufficiently approximate the data. The higher perisomatic branch density seems to be an essential feature to ensure sufficient connectivity between pairs of human neurons, as computed in (31), compensating for the smaller number of neighbors around a neuron than in mice.

The topological analysis was generalized to other cortical layers (layer 5) and brain regions (hippocampus) for which data were available. The topological examination of pyramidal cells from the layer 5 temporal cortex revealed the persistence of observed topological differences in deeper cortical layers. The dendritic branches of layer 5 human pyramidal (Fig S 3) cells exhibited a higher density in proximity to the soma, with branches commencing earlier

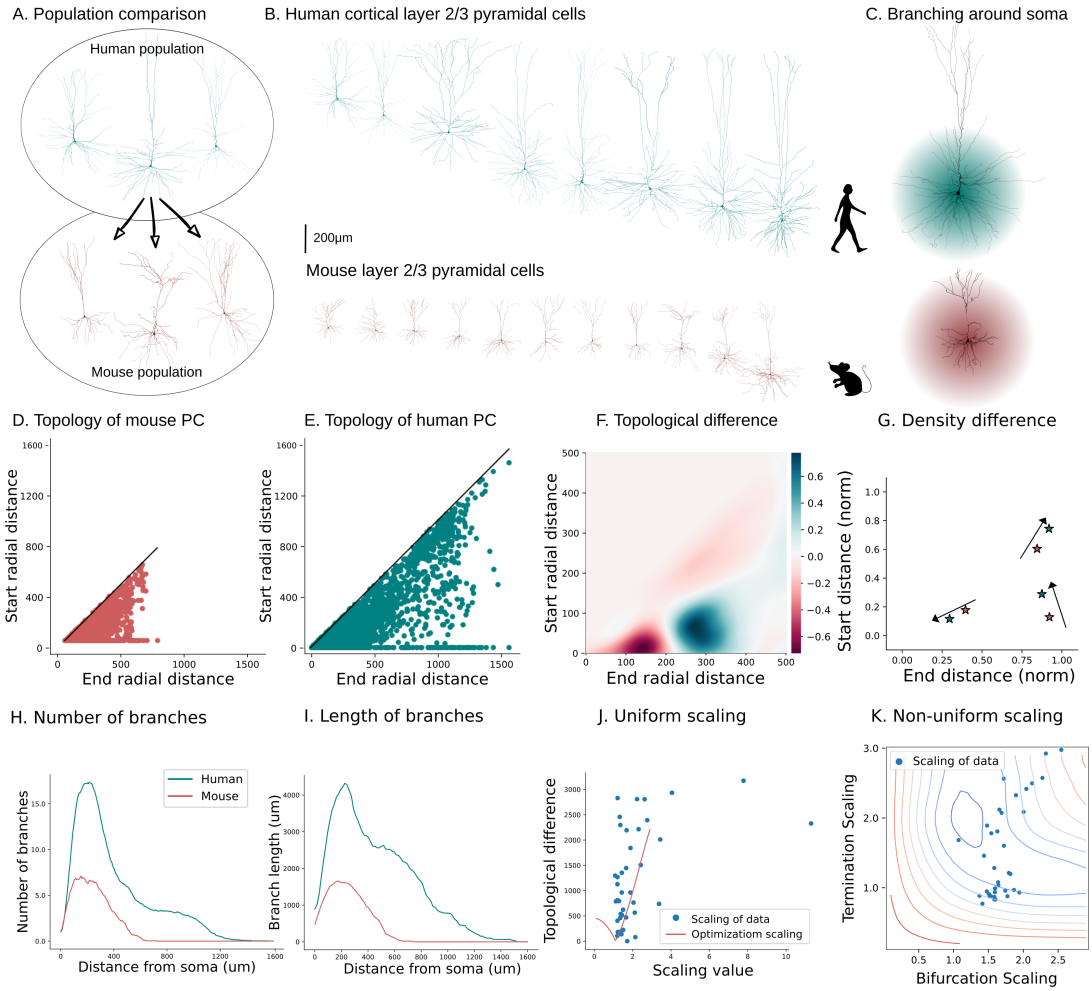

Figure 4: **Comparative topological analysis of layer 2 and 3 cortical pyramidal cells.** A. Schematic representation of the pairwise population comparison approach. B. Exemplary reconstructions of layer 2 and 3 cortical pyramidal cells in humans and mice. C. Schematic of topological branching around the neuronal soma for human and mouse. Human pyramidal cells express high branching density around the soma. D. Topological representation of mouse neurons. E. Topological representation of human neurons. F. Zoom-in of the topological differences around the soma demonstrating the area of maximum difference that is localized at $200 - 500\mu m$. G. The topological differences, cell sizes normalized to $(0 - 1)$, approximated by gaussian kernels for human (teal) and mouse (red). The arrows show direction of change at different dendritic compartments. H. Distribution of topological branches around neuronal soma. I. Distribution of lengths of topological branches. J. Uniform scaling (red curve) compared to experimental data (blue points). K. Non-uniform scaling (contour) compared to experimental data (blue points).

and extending further away from the soma than in mouse, confirming that the observed topological profiles of human cells extend to neurons beyond layers 2 and 3. Remarkably, these results also generalize to other brain regions. Data obtained from Benavides et al (18) in the mouse and human hippocampus (Fig S 3) demonstrated a similar pattern. This finding is particularly intriguing as it highlights a distinct single-cell characteristic that serves as a signature feature of human cells, with high branch densities localized at $200-500\mu m$ around neuronal somata.

A topological analysis performed on the dendrites of basket cells in layers 2 and 3 for human and mouse (Fig S 4) demonstrated that the observed topological differences between the two species persist in the dendrites of interneurons (Fig S 4). For this analysis, we focused on basket cells as they are the best characterized cell type of interneurons in the human brain. This analysis will be generalized to the highly diverse cortical interneuron types, once sufficient data become available (32). However, the higher density of branches around the somata of basket cells is significantly less prominent than the respective difference in branching density of pyramidal cells. This distinct topological pattern highlights a clear differentiation between pyramidal cells and interneurons within the cortical circuitry. Pyramidal cells' dendrites are not only larger in size, but also express high topological complexity around the soma, a feature that facilitates the generation of highly interconnected subnetworks in the human cortex. These findings further emphasize the complexity and diversity of neuronal architecture in the human brain and suggest that different cell types contribute to the overall network organization in distinct ways.

Increased memory capacity stems from increased dendritic complexity

The natural question that follows is whether the observed structural differences confer a computational advantage to the human brain. Numerous studies have supported the importance of dendritic complexity for computational capacity (33; 34; 35; 36). To address this question, we build upon research in dendritic impact (37) by calculating the anticipated memory capacity for a non-linear branching dendrite and comparing it with its topological complexity (Fig S 5). Memory capacity is defined as the number of possible combinations between the inputs of the dendrite and its non-linear components (see Methods Memory capacity). Topological complexity, in this context, refers to the entropy of bar lengths within the persistence barcode of a neuron (see Methods: Topological analysis). We observed that memory capacity is correlated with topological complexity (Fig S 5), as anticipated by the increased number of branches, enabling the sampling of a larger combination space for the synaptic inputs. The topological complexity of human pyramidal cells is greater than that in mice by a factor of 1.8, resulting in a corresponding enhancement in memory capacity by a factor of 1.7. These findings suggest that dendritic complexity serves as a suitable indicator

for predicting the expected memory capacity of individual neurons.

Cognitive enhancement hypothesis

Despite the greater inter-neuron distances resulting from lower neuron density in human pyramidal cells (Fig 5A-B), the distinct topology of their dendritic arbors (Fig 5C-D) emerges as a mechanism to establish higher-order interactions, as evidenced by the larger number of higher-dimensional simplices in the network (Fig 5E-F). In contrast, while interneurons exhibit higher densities in human, their simpler structural characteristics (32) limit their capacity to enhance network complexity to the same extent. These observations are supported by a balance in inhibition and excitation (21) in the innervation of pyramidal cells in the human cortex. These findings suggest that the intricate morphology of individual neurons can significantly influence the properties and characteristics of the networks they contribute to, providing strong evidence of a direct link between dendritic complexity and the overall structure of neuronal networks.

Two primary approaches to achieve higher-order complexity in neuronal networks are commonly proposed: increasing the number of nodes (38) or enhancing the complexity of individual nodes (39; 40). Interestingly, instead of simply adding more nodes, the human brain has evolved to prioritize the complexity of individual neurons, as observed in the morphological characteristics of human pyramidal cells. This suggests that the human brain has harnessed the potential of single-neuron complexity as a mechanism to create and support complex network connectivity, potentially conferring unique cognitive advantages.

Discussion

Topological analysis of human and mouse neurons revealed significant morphological differences between the two species. In particular, dendrites of human pyramidal cells exhibit a higher density of branches around the soma ($200 - 500\mu m$) than mouse dendrites. This distance corresponds to the increased empty space between neurons in the human cortex due to decreased neuronal density. The observed topological differences persist across cortical layers (layers 2, 3 and 5) and brain regions (hippocampus), suggesting they are a defining feature of human cells. We found that the distinctive perisomatic branching pattern exhibited by human dendrites serves as an effective compensatory mechanism for the increased inter-neuron distance, in order to preserve the density of dendritic processes and the connectivity between neurons.

Furthermore, the higher dendritic complexity in humans contributes to substantially higher numbers and dimensions of simplices in networks of human pyramidal cells, suggesting that dendritic morphology has considerable influence on how individual cells interconnect to form a network. The increased structural complexity generated by the sophisticated shapes

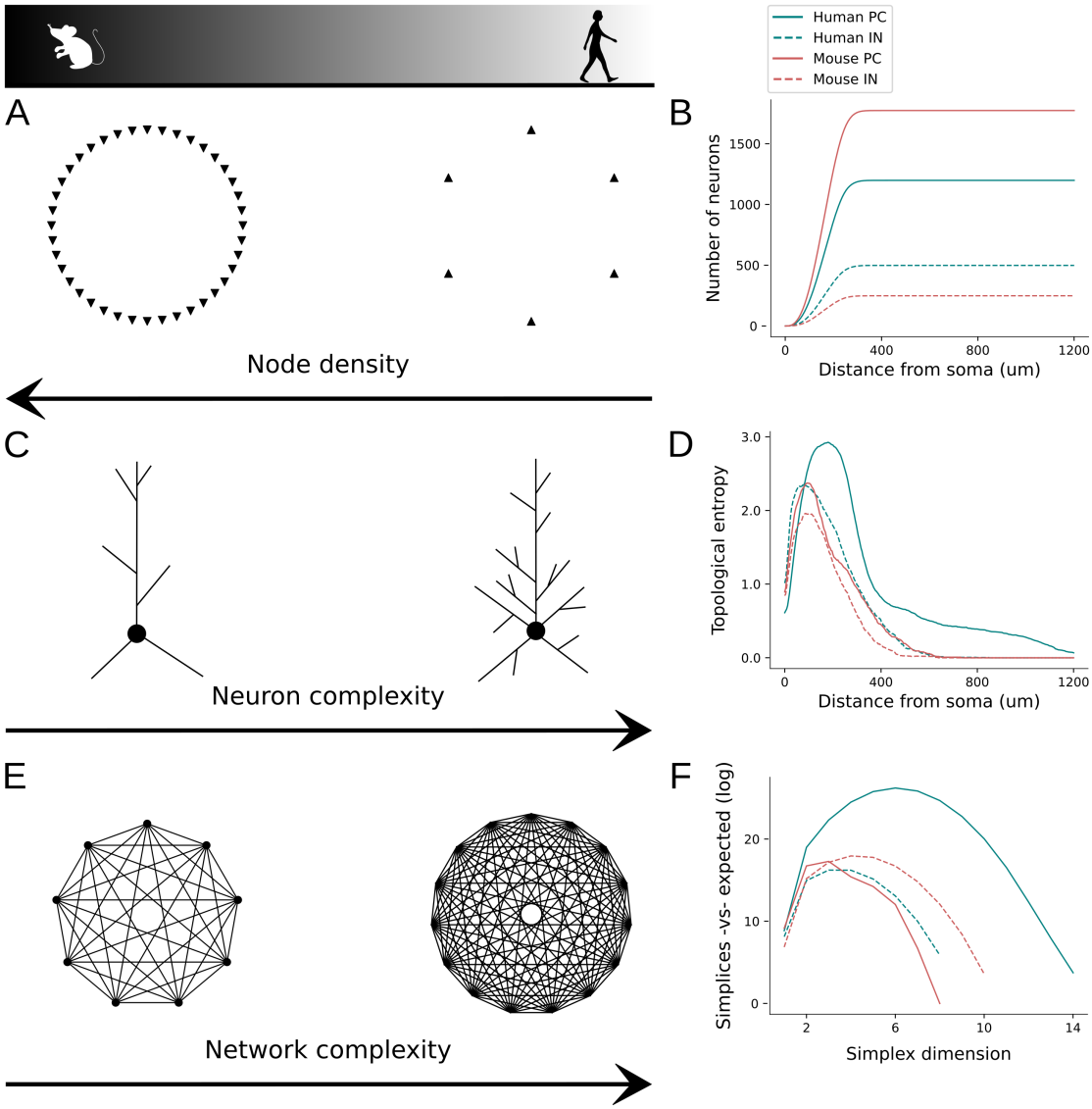

Figure 5: **Single-cell complexity influences networks complexity.** Human networks exhibit lower density of neurons (A) and therefore larger inter-neuron distances (B). However, human dendrites (and especially pyramidal cells) are highly complex (C-D). The combination of complex dendrites in human pyramidal cells and lower neuronal density generates highly complex human subnetworks (E-F). The effect of increased topological complexity of dendrites is a better indicator of network complexity as demonstrated by the highly interconnected subnetworks of pyramidal cells in the human (E-F), an effect that does not generalize to the less complex intereneuron subnetworks.

of dendrites suggests that a network is not merely a simple sum of its individual compo-

nents. The intricate branching patterns of human pyramidal cells potentially enable more robust and coordinated neural computations through the formation of highly interconnected subnetworks, represented by higher dimensional simplices. This result reinforces the view that dendritic complexity plays a crucial role in biological networks (35; 36), as proposed by Cajal (10).

Our analysis substantiates a compelling hypothesis that challenges the conventional notion of increasing node density as a means of optimizing the computational capacity of networks. Instead, we propose that enhancing node complexity, as observed in the distinct morphological features of human neurons, may be an alternative mechanism for optimizing network performance. The biological mechanism by which increased node complexity enhances the computational capabilities of a network remains an intriguing open question. However, it is not difficult to imagine that the simultaneous greater memory capacity within individual neurons and the substantially higher simplex counts should result in networks with higher computational power. As our understanding of the human neocortex continues to evolve, we anticipate that future models of the human cortex will integrate comprehensive information about cell types, transcriptomic and morpho-electrical relationships (16; 15), and preferential connectivity rules (17; 21) to create a more accurate understanding of the human brain.

The interplay between interneurons and pyramidal cells, as well as the functional role of each component within the network, is an important aspect that warrants further investigation. With the discovery of a larger proportion of interneurons in the human brain than in mouse, there has been speculation that they may have unforeseen functional significance (21). Our findings suggest that the simpler dendritic shapes of interneurons (32) may necessitate a higher abundance of these cells in order to maintain the balance between excitation and inhibition within the network. This suggestion is reinforced by experimental findings of preserved balance between inhibition and excitation as synaptic inputs of excitatory cells (21). Moreover, the sparsity of connections within the interneuron subnetwork implies that their role might primarily involve regulating the highly connected network of pyramidal cells. However, this finding cannot be generalized to all interneuron types, due to the great diversity in interneuron shapes (41; 42) and the specific roles of different types in the functionality of human networks (43). Our analysis focused primarily on the most abundant interneuron shapes, the basket-like cells. However further analysis is required to include more interneuron types, such as the bipolar-type interneurons, which prefer the innervation of other interneurons and have been found to form increased connections in the human (21). Therefore, exploring the connectivity patterns within the overall network of both excitatory and inhibitory cells, rather than focusing solely on their respective subnetworks, would provide valuable insights into the necessity for a greater number of interneurons and their specific contributions to network dynamics (43).

Methods

Experimental reconstructions

Human Brain Slice Preparation

All procedures were performed with the approval of the Medical Ethical Committee of the VU medical center (VUmc), and in accordance with Dutch license procedures and the Declaration of Helsinki. All patients provided written informed consent. Tissue was obtained from the idle temporal gyrus (MTG) during neurosurgical resection of non-pathological cortical tissue, to gain access to deeper lying pathology. Immediately upon resection, the tissue block was placed into a sealed container filled with ice-cold, artificial cerebral spinal fluid (aCSF) consisting of (in mM): 110 choline chloride, 26 NaHCO3, 10 D-glucose, 11.6 sodium ascorbate, 7 MgCl2, 3.1 sodium pyruvate, 2.5 KCl, 1.25 NaH2PO4 and 0.5 CaCl2. Before use, the aCSF solution was maintained carbogenated with 95% O2, 5% CO2 and the pH was adjusted to 7.3 by addition of 5M HCl solution.

The transition time between resection in the operation room and arriving at the neurophysiology lab was less than 20 minutes. Immediately upon arrival at the lab, the tissue block was cleaned of residual blood and after identifying the pia-white matter (WM) axis, pia was carefully removed. Subsequently, coronal slices of 350 µm-thick were made using a vibratome (Leica V1200S), in ice-cold aCSF solution. After recovering in a heat bath between 15-30 minutes at $34C$, the slices were kept for 1 hour at room temperature before recording in aCSF, which contained (in mM): 125 NaCl; 3 KCl; 1.2 NaH2PO4; 1 MgSO4; 2 CaCl2; 26 NaHCO3; 10 D-glucose (300 mOsm), bubbled with carbogen gas (95% O2/5% CO2). Borosilicate glass patch pipettes (Harvard apparatus/Science products GmbH) were filled with intracellular solution, containing (in mM): 115 K-gluconate, 10 HEPES, 4 KCl, 4 Mg-ATP, 10 K-Phosphocreatine, 0.3 GTP, 0.2 EGTA, and biocytin 5 mg/ml, pH adjusted to 7.3 with KOH, osmolarity 295 mOsm/kg). Using this intracellular, the recorded cell passively filled with biocytin during the patch clamp recording, allowing for subsequent staining of the cell.

Immunohistochemistry

Following whole cell patch-clamp recordings, slices were fixed in 4% paraformaldehyde (in phosphate buffer) for a minimum of two days. Then, biocytin-filled neurons were visualized using the chromogen 3,3-diaminobenzidine (DAB) tetrahydrochloride avidin–biotin–peroxidase method. In addition, a 4,6-diaminidino-2-phenylindole (DAPI) staining was performed. Slices were mounted on slides and embedded in mowiol (Clariant GmbH, Frankfurt am Main, Germany).

Morphological reconstruction

All recovered neurons underwent critical quality checks including assessment of staining quality and visualization, and occurrence of slicing artifacts (i.e. slicing plane not parallel to apical dendrites). Only neurons that passed quality control were reconstructed with Neurolucida software (Microbrightfield, Williston, VT, USA), using an 100x oil objective. From these 3D reconstructed neurons, morphological parameters could be extracted for further analysis.

Topological analysis

Algebraic topology provides mathematical tools to characterize geometric shapes by encoding features that persist across length scales. The Topological Morphology Descriptor (TMD, (27)) represents the branching structure of trees as a persistence barcode, encoding the start and end distances from the soma of each branch in the underlying structure as an interval in the real line.

Given a rooted tree T with a set of N branches that consist of terminations or leaves l and intermediate branching points or bifurcations b, and given a real-valued function f on the nodes of the tree, such as the Euclidean (or path) distance from the root R, the TMD algorithm generates a persistence barcode PB:

$$PB = \left\{(b_i, t_i) \mid i \leq N\right\} \tag{1}$$

Each bar (b_i, t_i) in the persistence barcode associates a branch in the tree T with a pair of real numbers: if the i^{textth} branch has bifurcation b and leaf l, then $b_i = f(b)$ and $t_i = f(l)$.

In brief, the persistence barcode is a set of intervals that encode the values of the function f at the start b and the end l of each branch. An equivalent representation of the persistence barcode is the corresponding persistence diagram PD, in which each interval of the barcode is encoded by the pair of its endpoints, seen as a point in the real plane.

There are many well known methods to generate vectorizations of persistence barcodes, from which one can then compute various statistics. For example, the persistence diagram can be converted to a finite-dimensional vector representation, the persistence image PI (44), which is essentially a sum of Gaussian kernels centered around the points in the persistence diagram.

Another useful vectorization of a persistence diagram or barcode is its topological entropy (45), which is computed from the lengths of the bars:

$$E(PB) = -\sum_{i}^{N} \frac{l_i}{L} \cdot log(\frac{l_i}{L}) \tag{2}$$

where $l_i = |t_i - b_i|$ is the length of each bar and $L = \sum_i^L l_i$ is the total length of all bars.

Topological scaling

The TMD associates a persistence diagram to any tree and thus to any reconstructed neuron morphology. Re-scaling a tree transforms the associated persistence diagram as follows. If T is a tree with a corresponding persistence barcode $PB = \{(b_i, t_i) \mid i \leq N\}$ given by the affine function f, the tree T' is obtained from T by linear, or uniform, scaling by a factor $\alpha > 0$ of all the branches, then its associated persistence barcode PB' is

$$PB' = \{(\alpha \cdot b_i, \alpha \cdot t_i) \mid i \leq N\}.$$

Note that the persistence entropy is scale-invariant as shown:

$$E(a \cdot PB) = -\sum_{i}^{N} \frac{a \cdot l_i}{a \cdot L} \cdot log(\frac{a \cdot l_i}{a \cdot L}) = -\sum_{i}^{N} \frac{l_i}{L} \cdot log(\frac{l_i}{L}) = E(PB) \tag{3}$$

If T is a tree with a corresponding persistence barcode PB as above, and the tree T'' is obtained from T by scaling by a pair of factors $\alpha, \beta > 0$ of all the branches, so that the bifurcations of the branches are scaled by α and the leaves by β, then its associated persistence barcode PB'' is

$$PB'' = \{(\alpha \cdot b_i, \beta \cdot t_i) \mid i \leq N\}.$$

Scaling optimization

In order to evaluate the scaling hypothesis, we have designed two experiments: the first one assumes uniform scaling through the morphology, and the second one non-uniform scaling as described above.

As a measure of the distance between two populations of cells, we computed the sum of the differences between the persistence images of the two populations, where the persistence image of a population is the sum of the persistence images of each cell in the population.

In the case of uniform scaling, we sought an optimal scaling factor $\alpha > 0$ that transforms the population of mouse cells to human cells, minimizing the distance between the two populations.

For the non-uniform scaling, we sought for two independent scaling factors $\alpha > 0$ and $\beta > 0$ to transform the population of mouse cells to human cells, minimizing the distance between the two populations.

In both cases, a gradient descent approach was implemented to identify the optimal factors. The results are presented in Fig 3D, along with the respective experimental data for comparison. Even though the identified optimal factors minimize the topological distances (difference between persistence images) between the two populations, they cannot capture the individual data points.

Computation of inter-neuron distances

The inter-neuron distances were computed in two ways: by a mathematical formula and by a simulation of points generated according to the selected density and the respective spatial dimension. For the mathematical formula, we used equation (4) from (46).

$$< R_v >= 0.554 \times N_v^{-1/3} \tag{4}$$

where $N_v = \frac{N}{V}$ is defined as the number of particles N per unit volume V.

The result was confirmed by the computational generation of 100 instances of uniform point processes and computing the average minimum distance within each set of points. The reported results correspond to the distance computed by the simulation, but the computation using the mathematical formula (4) yielded the same values.

Density of dendritic branches

Based on the total number of synapses within a cortical volume S_v and the density of synapses d_{syn} on the dendrites, the density d_{dend} of dendritic branches within a cortical volume is computed as:

$$d_{dend} = \frac{S_v}{d_{syn}} \tag{5}$$

Similarly, the density of axons can be computed by the bouton density d_{bouton}:

$$d_{axon} = \frac{S_v}{d_{bouton} * n_{syn_bouton}} \tag{6}$$

However, due to inconclusive experimental data about the number n_{syn_bouton} of synapses that correspond to each bouton, we were unable to provide an accurate measurement for the respective axon density.

In addition, the measurements of axonal lengths and bouton densities for individual neurons are difficult to assess experimentally, due to the inability of staining techniques to accurately stain the axonal processes that are further away from the soma. Therefore, the analysis of axonal data should be re-assessed once more accurate experimental data become available.

Memory capacity

Poirazi et al. (37) computed the memory capacity based on two different models: the linear model, which assumes dendritic inputs are summed linearly at the neuronal soma, and the non-linear model, which assumes the dendritic branches integrate the signal non-linearly.

Independent of the choice of non-linearity introduced on the dendrites, memory capacity increases significantly if non-linearities are taken into account.

Given a dendrite with m branches, each branch contains k excitatory inputs, thus $s = mk$ synaptic contacts and a set of d dendritic inputs, the memory capacity can be computed as follows.

For the linear model, the computed memory capacity is:

$$C_L = 2log_2\binom{s+d-1}{s} \tag{7}$$

Note that in this case, the number of branches m and their synaptic length k are not relevant for the computation of the memory capacity.

For the non-linear model, the computed memory capacity is:

$$C_N = 2log_2\binom{\binom{k+d-1}{k}+m-1}{m} \tag{8}$$

On the contrary, for the non-linear model, the distribution of synaptic lengths k on the m branches plays a crucial role in the memory capacity of the dendrite. As shown in Fig 5B the memory capacity increases with the number of branches, due to the increased number of ways to combine the dendritic inputs. The number of branches here corresponds to the number of computational subunits in the dendritic tree (47), rather than the physical branches of the tree.

Computation of appositions

The appositions between a pair of neurons were quantified as the number of "contact points" where the pre-synaptic axons approach the post-synaptic dendrites within a distance of $2\mu m$. It is important to note that these contact points do not directly represent synaptic connections, but rather indicate potential sites for synapse formation. Therefore the results presented on appositions should be interpreted as a measure of the likelihood of synaptic connections between neurons.

The detailed methodology for the computation of the appositions is described in (24).

Computation of simplex distribution

Recent advances in algebraic topology (25; 24) have introduced a powerful tool for comprehending network complexity - the computation of cliques and cavities formed by the underlying graph. This approach allows for a deeper understanding of the intricate connections and structures within networks, enabling researchers to unveil hidden patterns and gain insights into their organizational principles.

The dimension of a clique in a network is one less than the number of neurons of which it is composed; higher dimensions indicate higher complexity. In directed graphs, directed cliques are of particular significance as they comprise a single source neuron and a single sink neuron, representing a distinct pattern of connectivity, with the potential to influence the flow of activity within the network, making it an important consideration in network analysis (48; 29).

To bring the connection probability within a reasonable range, we applied a random reduction of 50% to the connectivity matrix formed by the appositions between neurons. This adjustment aimed to ensure a more realistic representation of the network by reducing excessive connections. The mouse and human networks were partitioned into distinct excitatory and inhibitory subnetworks. For each subnetwork, we computed the connection probability and analyzed the distribution of simplices, allowing us to assess the network characteristics and topological complexity specific to each subpopulation.

Data availability

The data and the code used in this study will become available upon request after publication. The topological analysis was performed using https://github.com/BlueBrain/TMD. The morphological analysis was performed using https://github.com/BlueBrain/NeuroM.

Author contributions

L.K. conceived and supervised the study, designed the computational experiments, performed analysis, and wrote the manuscript. Y.S. supervised, performed, and validated reconstructed neurons. A.A. analyzed neuronal morphologies and generated neuronal networks. N.B. collected and revised literature information. R.B.P. reconstructed neurons and provided synaptic data for the human and mouse cortex and hippocampus. J.C. edited the manuscript. J.D.F. provided anatomical and connectivity data for the human and mouse cortex. K.H. designed the topological methods and edited the manuscript. H.D.M. provided anatomical data for the human cortex. E.J.M. performed experiments and reconstructed human neurons. I.S. supervised the study. H.M. supervised the study and provided funding. C.P.J.d.K. provided data and supervised the study. J.M. contributed with histological preparations. R.P. and M.P. contributed with electrophysiological recordings of interneurons. R.T.D. and R.S. provided the human tissue for LNMC reconstructions. All authors reviewed the paper and discussed the results at all stages of this study.

Acknowledgements

The authors thank Daniela Egas-Santader for her useful contributions to the efficient computation of simplices in the generated networks. This study was supported by funding to the Blue Brain Project, a research center of the École polytechnique fédérale de Lausanne (EPFL), from the Swiss government's ETH Board of the Swiss Federal Institutes of Technology.

References

[1] Cairò, O. External measures of cognition. *Frontiers in Human Neuroscience* **5** (2011).

[2] Hart, B. L., (Geyer), L. A. H., McCoy, M. C. & Sarath, C. R. Cognitive behaviour in asian elephants: use and modification of branches for fly switching. *Animal Behaviour* **62**, 839–847 (2001).

[3] Waugh, D. A. & Thewissen, J. G. M. The pattern of brain-size change in the early evolution of cetaceans. *PLoS ONE* **16** (2021).

[4] Hofman, M. A. Size and shape of the cerebral cortex in mammals. ii. the cortical volume. *Brain, behavior and evolution* **32 1**, 17–26 (1988).

[5] Herculano-Houzel, S. The human brain in numbers: A linearly scaled-up primate brain. *Frontiers in Human Neuroscience* **3** (2009).

[6] Menary, K. R. *et al.* Associations between cortical thickness and general intelligence in children, adolescents and young adults. *Intelligence* **41 5**, 597–606 (2013).

[7] Hopkins, W. D., Hopkins, W. D., Li, X. & Roberts, N. More intelligent chimpanzees (pan troglodytes) have larger brains and increased cortical thickness. *Intelligence* (2019).

[8] Gregory, M. D. *et al.* Regional variations in brain gyrification are associated with general cognitive ability in humans. *Current Biology* **26**, 1301–1305 (2016).

[9] Galakhova, A. *et al.* Evolution of cortical neurons supporting human cognition. *Trends in Cognitive Sciences* **26**, 909–922 (2022).

[10] y Cajal, S. R. Histologie du système nerveux de lhomme et des vertébrés. *Journal of Neuropathology and Experimental Neurology* **57**, 883 (1998).

[11] DeFelipe, J., Alonso-Nanclares, L. & Arellano, J. I. Microstructure of the neocortex: Comparative aspects. *Journal of Neurocytology* **31**, 299–316 (2002).

[12] Mohan, H., Verhoog, M. B., Doreswamy, K. K., Eyal, G. & et al., R. A. Dendritic and axonal architecture of individual pyramidal neurons across layers of adult human neocortex. *Cerebral Cortex (New York, NY)* **25**, 4839 – 4853 (2015).

[13] Deitcher, Y. *et al.* Comprehensive morpho-electrotonic analysis shows 2 distinct classes of l2 and l3 pyramidal neurons in human temporal cortex. *Cerebral Cortex (New York, NY)* **27**, 5398 – 5414 (2017).

[14] Beaulieu-Laroche, L. *et al.* Allometric rules for mammalian cortical layer 5 neuron biophysics. *Nature* **600**, 274 – 278 (2021).

[15] Berg, J., Sorensen, S. A., Ting, J. T., Miller, J. A. & et al., T. C. Human neocortical expansion involves glutamatergic neuron diversification. *Nature* **598**, 151 – 158 (2021).

[16] Bakken, T. E. *et al.* Single-cell and single-nucleus rna-seq uncovers shared and distinct axes of variation in dorsal lgn neurons in mice, non-human primates, and humans. *eLife* **10** (2021).

[17] Kalmbach, B. E., Hodge, R. D., Jorstad, N. L., Owen, S. F. & de Frates et al., R. Signature morpho-electric, transcriptomic, and dendritic properties of human layer 5 neocortical pyramidal neurons. *Neuron* **109**, 2914–2927.e5 (2021).

[18] Benavides-Piccione, R. *et al.* Differential structure of hippocampal ca1 pyramidal neurons in the human and mouse. *Cerebral cortex* (2019).

[19] Rollenhagen, A. *et al.* Synaptic organization of the human temporal lobe neocortex as revealed by high-resolution transmission, focused ion beam scanning, and electron microscopic tomography. *International Journal of Molecular Sciences* **21** (2020).

[20] Cano-Astorga, N., DeFelipe, J. & Alonso-Nanclares, L. Three-dimensional synaptic organization of layer iii of the human temporal neocortex. *Cerebral Cortex (New York, NY)* **31**, 4742 – 4764 (2021).

[21] Loomba, S. *et al.* Connectomic comparison of mouse and human cortex. *Science* **377** (2022).

[22] Cano-Astorga, N., Plaza-Alonso, S., DeFelipe, J. & Alonso-Nanclares, L. 3d synaptic organization of layer iii of the human anterior cingulate and temporopolar cortex. *bioRxiv* (2023).

[23] Benavides-Piccione, R., Ballesteros-Yáñez, I., DeFelipe, J. & Yuste, R. Cortical area and species differences in dendritic spine morphology. *Journal of Neurocytology* **31**, 337–346 (2002).

[24] Reimann, M. W. *et al.* Cliques of neurons bound into cavities provide a missing link between structure and function. *Frontiers in Computational Neuroscience* **11** (2017).

[25] Sizemore, A. E. *et al.* Cliques and cavities in the human connectome. *Journal of Computational Neuroscience* **44**, 115 – 145 (2016).

[26] DeFelipe, J. The evolution of the brain, the human nature of cortical circuits, and intellectual creativity. *Frontiers in Neuroanatomy* **5** (2011).

[27] Kanari, L. *et al.* A topological representation of branching neuronal morphologies. *Neuroinformatics* **16**, 3–13 (2018).

[28] Gal, E. *et al.* The role of hub neurons in modulating cortical dynamics. *Frontiers in Neural Circuits* **15** (2021).

[29] Nolte, M., Gal, E., Markram, H. & Reimann, M. W. Impact of higher order network structure on emergent cortical activity. *Network Neuroscience* **4**, 292 – 314 (2019).

[30] Hodge, R. D., Bakken, T. E., Miller, J. A., Smith, K. A. & et al., E. R. B. Conserved cell types with divergent features in human versus mouse cortex. *Nature* **573**, 61 – 68 (2019).

[31] Hunt, S., Leibner, Y., Mertens, E. J., Barros-Zulaica, N. & et al., L. K. Strong and reliable synaptic communication between pyramidal neurons in adult human cerebral cortex. *Cerebral Cortex (New York, NY)* **33**, 2857 – 2878 (2022).

[32] Wilbers, R. *et al.* Structural and functional specializations of human fast-spiking neurons support fast cortical signaling. *Science Advances* **9**, eadf0708 (2023).

[33] Segev, I. Sound grounds for computing dendrites. *Nature* **393**, 207–208 (1998).

[34] Koch, C. & Segev, I. The role of single neurons in information processing. *Nature Neuroscience* **3 Suppl 1**, 1171–1177 (2000).

[35] Häusser, M. & Mel, B. W. Dendrites: bug or feature? *Current Opinion in Neurobiology* **13**, 372–383 (2003).

[36] Larkum, M. E. Are dendrites conceptually useful? *Neuroscience* **489**, 4–14 (2022).

[37] Poirazi, P. & Mel, B. W. Impact of active dendrites and structural plasticity on the memory capacity of neural tissue. *Neuron* **29**, 779–796 (2001).

[38] Jang, J., Cho, H., Kim, J., Lee, J. & Yang, S. Deep neural networks with a set of node-wise varying activation functions. *Neural networks : the official journal of the International Neural Network Society* **126**, 118–131 (2020).

[39] Zhang, Z. & fei Qiao, J. A node pruning algorithm for feedforward neural network based on neural complexity. *2010 International Conference on Intelligent Control and Information Processing* 406–410 (2010).

[40] Pagkalos, M., Chavlis, S. & Poirazi, P. Dendrify: a new framework for seamless incorporation of dendrites in 1 spiking neural networks (2022).

[41] Chartrand, T., Dalley, R., Close, J., Goriounova, N. A. & et al., B. R. L. Morphoelectric and transcriptomic divergence of the layer 1 interneuron repertoire in human versus mouse neocortex. *bioRxiv* (2022).

[42] Lee, B. R. *et al.* Signature morpho-electric properties of diverse gabaergic interneurons in the human neocortex. *bioRxiv* (2022).

[43] Yao, H. K. *et al.* Reduced inhibition in depression impairs stimulus processing in human cortical microcircuits. *bioRxiv* (2021).

[44] Adams, H. *et al.* Persistence images: A stable vector representation of persistent homology. *J. Mach. Learn. Res.* **18**, 8:1–8:35 (2015).

[45] Chintakunta, H., Gentimis, T., Gonzalez-Diaz, R., Jiménez, M. J. & Krim, H. An entropy-based persistence barcode. *Pattern Recognit.* **48**, 391–401 (2015).

[46] Bansal, P. P. & Ardell, A. J. Average nearest neighbor distances between uniformly distributed finite particles. topical report (1971).

[47] Polsky, A., Mel, B. W. & Schiller, J. Computational subunits in thin dendrites of pyramidal cells. *Nature Neuroscience* **7**, 621–627 (2004).

[48] Perin, R., Berger, T. K. & Markram, H. A synaptic organizing principle for cortical neuronal groups. *Proceedings of the National Academy of Sciences* **108**, 5419 – 5424 (2011).

[49] Markram, H., Muller, E., Ramaswamy, S. & et al., M. W. R. Reconstruction and simulation of neocortical microcircuitry. *Cell* **163**, 456–492 (2015).

[50] Benavides-Piccione, R., Fernaud-Espinosa, I., Robles, V., Yuste, R. & DeFelipe, J. Age-based comparison of human dendritic spine structure using complete three-dimensional reconstructions. *Cerebral cortex* **23 8**, 1798–810 (2013).